ChemComm

COMMUNICATION

View Article Online
View Journal | View Issue

Cite this: *Chem. Commun.*, 2020, **56**, 1685

Received 21st September 2019,
Accepted 4th January 2020

DOI: 10.1039/c9cc07421j

rsc.li/chemcomm

On-surface synthesis of graphyne nanowires through stepwise reactions†

Xin Yu,‡ Liangliang Cai,‡ Meiling Bao, Qiang Sun, Honghong Ma, Chunxue Yuan * and Wei Xu *

From an interplay of high-resolution UHV-STM imaging and DFT calculations, we have achieved on-surface synthesis of graphyne nanowires through stepwise reactions involving two different types of dehalogenative homocoupling reactions (*i.e.*, C(sp^3)–Br and C(sp^2)–Br). This study would further supplement our database of on-surface synthesis and provide us with an alternative and efficient strategy for the fabrication of desired nanostructures/nanomaterials.

In recent years, on-surface synthesis has been a powerful tool to achieve atomically precise fabrication of well-defined nanostructures with applications in sensor devices, optoelectronics and molecular machines.[1–5] A variety of chemical reactions have been introduced on surfaces,[6–10] and among others, stepwise reactions have been proven to be a promising route for creating sophisticated molecular nanostructures, particularly, carbon nanostructures, *e.g.*, graphene nanoribbons, in which the on-surface dehalogenative homocoupling and subsequent dehydrogenative cyclization reactions are involved.[11–15] In such a stepwise reaction, different functional groups are sequentially activated by controlling specific experimental conditions.[16–21] Recently, we have illustrated the on-surface formation of polyphenyl chains through a stepwise reaction (*i.e.*, Ullmann coupling together with dehydrogenative homocoupling reactions), in which the same hybridized carbon atoms (*i.e.*, C-(sp^2)–Br and C-(sp^2)–H) are involved as the reaction sites.[22] While, to our knowledge, stepwise reactions involving two different types of hybridized carbon atoms have been less discussed so far. Therefore, it is of general interest to design such a stepwise reaction involving different types of dehalogenative homocoupling reactions (*e.g.*, C(sp^3)–Br and C(sp^2)–Br) on surfaces.

Very recently, we have achieved the direct formation of C–C triple bonded structural motifs by the on-surface dehalogenative homocouplings of tribromomethyl molecules.[23] In view of the successful *in situ* formation of the C–C triple bond from the sp^3 hybridized carbon, we have further functionalized the molecular precursor (1-bromo-4-(tribromomethyl)benzene, shortened as BTBMB, synthesis details and NMR spectra are shown in ESI†) with both the tribromomethyl and aryl bromide groups as shown in Scheme 1, and with the aim of introducing two types of dehalogenative homocoupling reactions (*i.e.*, C(sp^3)–Br and C(sp^2)–Br). From the interplay of high-resolution scanning tunneling microscopy (STM) imaging and density functional theory (DFT) calculations, we have investigated the dehalogenative homocouplings of BTBMB molecules on both Au(111) and Ag(110) surfaces. It has been demonstrated that by delicately controlling the substrate temperature, the tribromomethyl and aryl bromide groups could be sequentially activated resulting in a stepwise dehalogenative homocoupling reaction on surfaces, which leads to the formation of linear graphyne wire-like structures on both Au(111) and Ag(110) surfaces (*cf.* Scheme 1). Moreover, we have also introduced the (tribromomethyl)benzene molecule (shortened as TBMB, only with the tribromomethyl group) onto the Ag(110) surface to unravel the underlying mechanism of on-surface dehalogenative homocoupling reactions. This study exhibits the feasibility of on-surface stepwise dehalogenative C–C homocoupling reactions; and more importantly, it provides an alternative and efficient strategy for the fabrication of sophisticated surface nanostructures.

After the deposition of BTBMB molecules on Au(111) at RT, we have observed the formation of island structures as shown in Fig. 1a. From the close-up STM image shown in Fig. 1b, we identify that the formed dimer structure (indicated by the white contour) is composed of two lobes and a dim contrast in the center. To further identify the atomic scale structure, we perform extensive DFT calculations. From a detailed comparison of the experimental morphology and dimensions with the DFT-relaxed molecular model (*cf.* Fig. 1b and c), we could identify that the rod-like structure should be assigned to a C–C triple bonded dimer, while the aryl bromide groups still remain intact. The DFT-relaxed model is overlaid on the STM

Interdisciplinary Materials Research Center, College of Materials Science and Engineering, Tongji University, Shanghai 201804, P. R. China.
E-mail: cxyuan@tongji.edu.cn, xuwei@tongji.edu.cn

† Electronic supplementary information (ESI) available. See DOI: 10.1039/c9cc07421j

‡ X. Yu and L. Cai contributed equally to this work.

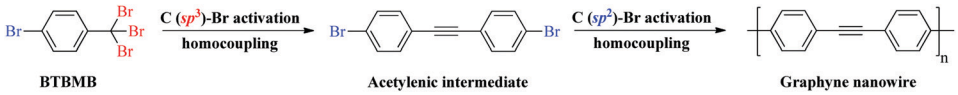

Scheme 1 The schematic illustration shows the stepwise dehalogenative homocoupling reactions, which results in the formation of a graphyne nanowire.

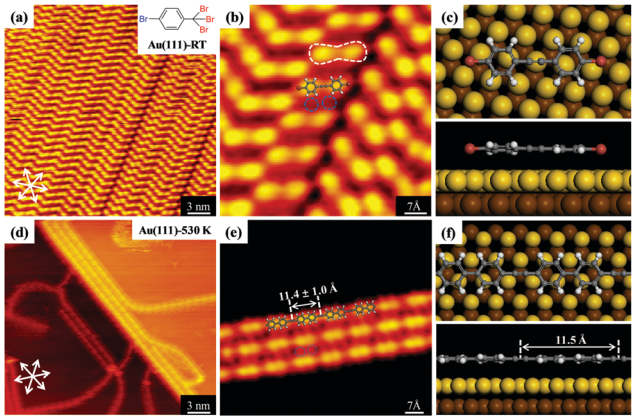

Fig. 1 (a) Large-scale and (b) close-up STM images showing the formation of a dimer structure after deposition of BTBMB molecules on Au(111) held at RT. The equally scaled DFT model is overlaid on the corresponding STM topography. (c) Top and side views of the DFT optimized model of the dimer structure on Au(111). (d) Large-scale and (e) close-up STM images showing the formation of graphyne nanowires after annealing the sample to ~530 K. The equally scaled DFT model is overlaid on the corresponding STM topography. The detached Br atoms are indicated by blue circles in (b) and (e). (f) Top and side views of the DFT optimized model of the graphyne nanowire on Au(111).

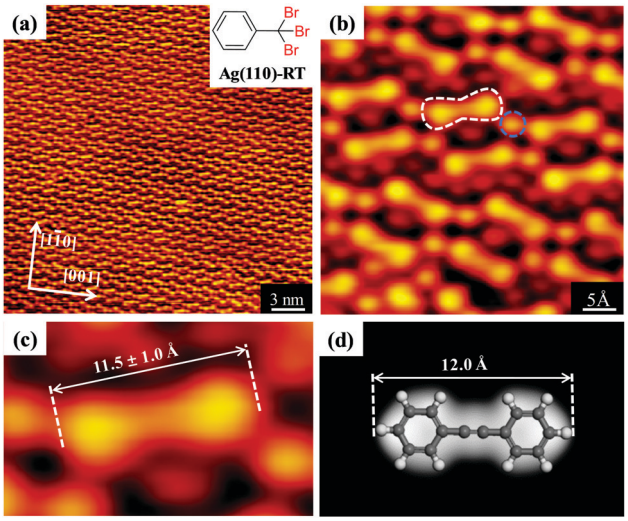

Fig. 2 (a) Large-scale and (b) close-up STM images showing the formation of an ordered island structure after deposition of TBMB molecules on Ag(110) held at RT. The STM topography of a dimer product is indicated by the white contour, and the round protrusions are highlighted by a blue circle. (c) The high-resolution STM image and (d) the corresponding simulated STM image overlaid by an equally scaled DFT relaxed structure of the dimer motif on Ag(110).

image for comparison (Fig. 1b). Remarkably, the straight morphology of the dimer structure together with the characteristic STM contrast[24–27] (*i.e.*, the middle part is apparently lower than those of the phenyl groups) implies the formation of the C–C triple bond. It is known that the aryl bromide group remains intact on Au(111) at RT,[28–30] which was also confirmed by XPS in this case as shown in the ESI.† Thus, we conclude that we have formed the C–C triple bonded dimer structure on Au(111). To trigger the aryl bromide group in the next step, we annealed the sample to ~530 K. Interestingly, we have observed the formation of graphyne nanowires as shown in Fig. 1d and e. A detailed comparison between the experimental morphology and dimensions and the DFT-relaxed model (Fig. 1e and f) allows us to confirm the formation of graphyne nanowires on the surface; in particular, some wires could extend over 30 nm along the step edges. Through the sequential C–C couplings, we have successfully formed a graphyne nanowire (*i.e.*, a kind of poly(aryleneethynylene) molecular chain), which is in analogy to the previously reported graphdiyne nanowire on the surface.[31,32]

To systematically study the stepwise reactions in detail, we have performed complementary experiments on Ag(110). We start with the TBMB molecule, only functionalized with a tribromomethyl group. After the deposition of TBMB molecules on Ag(110) held at RT, we observe the formation of ordered islands as shown in Fig. 2a, which consists of round protrusions and rod-like structures. According to the previous studies,[33–35] the round protrusions (highlighted by a blue cycle in Fig. 2b) are attributed to dissociated bromine atoms on the surface. The rod-like structure (indicated by the white contour in Fig. 2b) is composed of two lobes and a dim contrast in the center. Notably, the dimer made of TBMB molecules is in analogy to the one made of BTBMB molecules shown above. To further identify the atomic scale structure, we perform extensive DFT calculations. From a detailed comparison of the experimental morphology and dimensions with the molecular model and the simulated STM image (*cf.* Fig. 2c and d), we could identify that the rod-like structure should be assigned to a C–C triple bonded dimer. Note that deposition of TBMB molecules on Ag(110) held at lower temperatures (~250 K) also results in the formation of C–C triple bonded dimer structures.

To unravel the reaction mechanism on the formation of the C–C triple bonded dimer structure, we have calculated the reaction pathway from the molecular precursor to the dimer structure through successive C–Br bond activations and subsequent C–C couplings, which is in analogy to the dehalogenative homocoupling reaction of *gem*-dibromides.[36,37] Note that the TBMB molecule is evaporated from the crucible at RT, so it is unlikely for the molecules to be debrominated in the crucible or in the gas phase during evaporation. As shown in Fig. 3a, the split of the first C–Br bond is nearly spontaneous on the Ag(110)

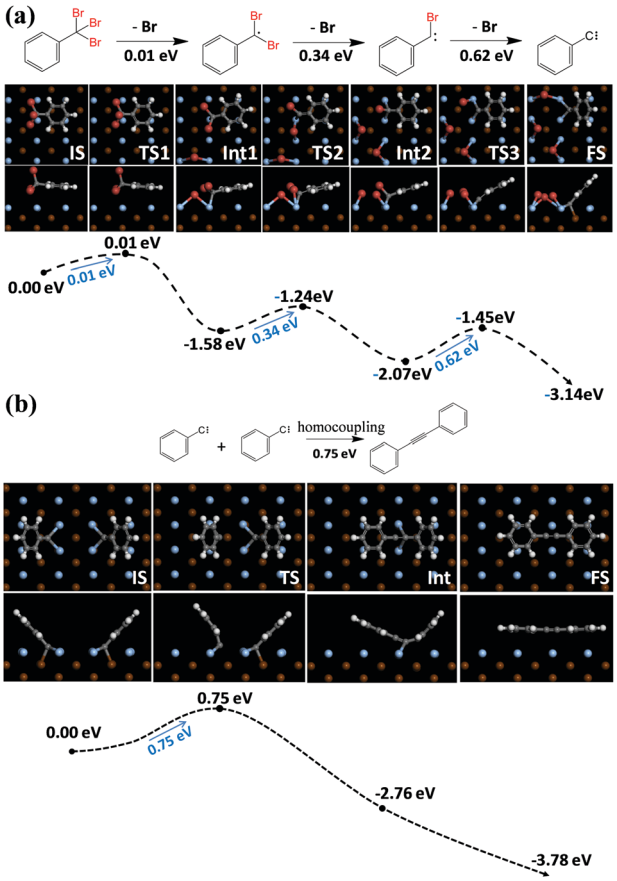

Fig. 3 (a) The DFT-calculated reaction pathway for the successive C–Br bond activations of the TBMB molecule on Ag(110). The structural models of the initial (IS), transition (TS), intermediate (Int) and final states (FS) along the pathway are also shown. (b) The DFT-calculated reaction pathway from the debrominated intermediates to the dimer product. The corresponding structural models along the pathways are also shown.

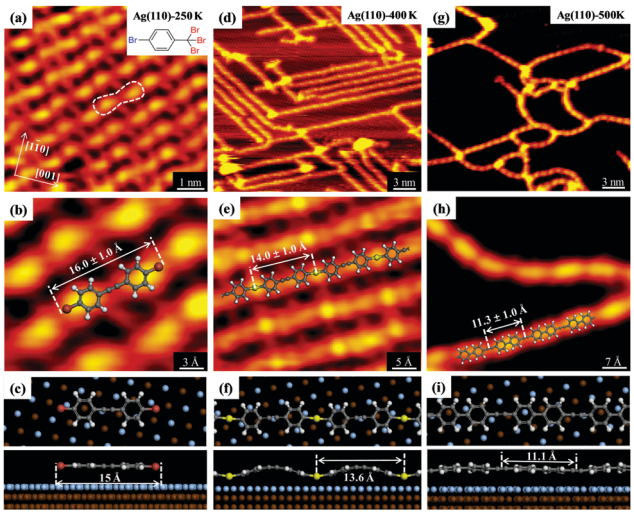

Fig. 4 (a) Large-scale and (b) close-up STM images showing the formation of a dimer structure after deposition of BTBMB molecules on Ag(110) held at ~250 K. The equally scaled DFT model is overlaid on the corresponding STM topography. (c) Top and side views of the DFT optimized model of the dimer structure on Ag(110). (d) Large-scale and (e) close-up STM images showing the formation of an organometallic chain structure after annealing the sample to ~400 K. The equally scaled DFT model is overlaid on the corresponding STM topography. (f) Top and side views of the DFT optimized model of the organometallic chain on Ag(110). (g) Large-scale and (h) close-up STM images showing the formation of graphyne nanowires after annealing the sample to ~500 K. The equally scaled DFT model is overlaid on the corresponding STM topography. (i) Top and side views of the DFT optimized model of the graphyne nanowire on Ag(110).

surface, which is comparable to the debromination of the bromomethyl group.[37] The energy barriers for the following debromination processes are determined to be 0.34 eV and 0.62 eV, respectively. The whole debromination reaction is exothermic by 3.14 eV. Then, we have calculated the energy barrier for the subsequent C–C couplings of the fully debrominated species, and the barrier was calculated to be 0.75 eV as shown in Fig. 3b, along with the reaction energy of 3.78 eV. Thus, these calculated energy barriers could well account for the formation of the C–C triple bonded dimer product under the experimental conditions (*cf.* ESI†).

A step further to explore the generality of on-surface synthesis of graphyne nanowires by the above stepwise reactions, we performed comparative studies to extend this approach by introducing BTBMB molecules onto the Ag(110) surface. As shown in Fig. 4a, after the deposition of BTBMB molecules on Ag(110) held at ~250 K, only the tribromomethyl group is triggered. From the STM images in Fig. 4a and b, we identify that the island also consists of dimer structures (as highlighted by a white contour in Fig. 4a) and bromine atoms. From the close-up STM image shown in Fig. 4b, we identify that the formed dimer structure is characteristically the same as the one formed by BTBMB molecules on Au(111) (*cf.* Fig. 1a and b) both in morphology and dimensions. Moreover, to further identify the atomic-scale structure of this dimer product, we also performed DFT calculations by constructing possible structures. From a detailed comparison of the experimental morphology and dimensions with the equally scaled relaxed model (*cf.* Fig. 4b and c), we conclude that the dimer structure should be assigned to a C–C triple bonded product, while the aryl bromide groups still remain intact. Then, we further annealed the sample to trigger the aryl bromide groups.

After annealing the sample to ~400 K, we observe the formation of chain structures on the surface as shown in Fig. 4d. From the close-up STM image (Fig. 4e), we could distinguish the formation of C–Ag–C organometallic chains, which is known for Ullmann-type reactions on the surface.[38] The Ag atoms show sharp contrasts within the chains, and the detached bromine atoms are aligned between the chains. Based on the above observation, we construct the molecular model of the organometallic chain and perform DFT calculations as shown in Fig. 4f. An equally scaled model of an organometallic chain is overlaid on the STM image (Fig. 4e), where a good agreement in both dimension and morphology is achieved. Further annealing the sample to ~500 K results in the formation of C–C coupled molecular chains with alternating acetylenic linkages and biphenyl groups as shown in Fig. 4g. From the

close-up STM image (Fig. 4h) and in comparison with the organometallic chain (Fig. 4e), we identify that the bright protrusions within the chains disappear, which implies the release of Ag atoms. We then optimized the model of the C–C coupled molecular chain on Ag(110) as shown in Fig. 4i. The equally scaled model is overlaid on the STM image (Fig. 4h), where a good agreement in both dimension and morphology is also achieved. Note that the bends should be due to the flexibility of the molecular wires, and for some specific junctions it may not be easy to unambiguously distinguish the exact structure. We speculate that this might be due to some side-reactions.

Furthermore, we also performed experiments on two different surfaces, *i.e.* Cu(111) and Cu(110), to explore the generality of the formation of graphyne nanowires. The polymerization outcomes were rather similar to the case of Au(111) and Ag(110), as shown in the ESI.†

In conclusion, from a combination of high-resolution UHV-STM imaging and DFT calculations, we have successfully achieved the on-surface synthesis of graphyne nanowires through stepwise reactions involving two different types of dehalogenative homo-coupling reactions (*i.e.*, C(sp^3)–Br and C(sp^2)–Br). This strategy would further supplement our database with on-surface synthesis and may shed light on the construction of sophisticated carbon nanostructures/nanomaterials with acetylenic scaffoldings from pre-designed molecular precursors.

The authors acknowledge financial support from the National Natural Science Foundation of China (21622307, 21790351) and the Fundamental Research Funds for the Central Universities.

Conflicts of interest

There are no conflicts to declare.

Notes and references

1 K. Leng, I. Abdelwahab, I. Verzhbitskiy, M. Telychko, L. Chu, W. Fu, X. Chi, N. Guo, Z. Chen, Z. Chen, C. Zhang, Q. H. Xu, J. Lu, M. Chhowalla, G. Eda and K. P. Loh, *Nat. Mater.*, 2018, **17**, 908.
2 Y. Isshiki, Y. Matsuzawa, S. Fujii and M. Kiguchi, *Micromachines*, 2018, **9**, 67.
3 W. R. Browne and B. L. Feringa, *Nat. Nanotechnol.*, 2006, **1**, 25.
4 V. Balzani, A. Credi, F. M. Raymo and J. F. Stoddart, *Angew. Chem., Int. Ed.*, 2000, **39**, 3348.
5 *On-Surface Synthesis*, ed. A. Gourdon, Springer International Publishing, Switzerland, 2014.
6 Q. Fan, J. M. Gottfried and J. Zhu, *Acc. Chem. Res.*, 2015, **48**, 2484.
7 P. A. Held, H. Fuchs and A. Studer, *Chem. – Eur. J.*, 2017, **23**, 5874.
8 F. Klappenberger, Y. Q. Zhang, J. Björk, S. Klyatskaya, M. Ruben and J. V. Barth, *Acc. Chem. Res.*, 2015, **48**, 2140.
9 L. Dong, P. N. Liu and N. Lin, *Acc. Chem. Res.*, 2015, **48**, 2765.
10 H. Zhang and L. Chi, *Adv. Mater.*, 2016, **28**, 10492.
11 C. Pigot and F. Dumur, *Materials*, 2019, **12**, 662.
12 N. Merino-Díez, A. P. Paz, J. Li, M. Vilas-Varela, J. Lawrence, M. S. G. Mohammed, A. Berdonces-Layunta, A. Barragán, J. I. Pascual, J. Lobo-Checa, D. Peña and D. G. de Oteyza, *ChemPhysChem*, 2019, **20**, 2305.
13 J. Cai, P. Ruffieux, R. Jaafar, M. Bieri, T. Braun, S. Blankenburg, M. Muoth, A. P. Seitsonen, M. Saleh, X. Feng, K. Müllen and R. Fasel, *Nature*, 2010, **466**, 470.
14 P. H. Jacobse, A. van den Hoogenband, M. E. Moret, R. J. M. K. Gebbink and I. Swart, *Angew. Chem., Int. Ed.*, 2016, **55**, 13052.
15 G. D. Nguyen, H. Z. Tsai, A. A. Omrani, T. Marangoni, M. Wu, D. J. Rizzo, G. F. Rodgers, R. R. Cloke, R. A. Durr, Y. Sakai, F. Liou, A. S. Aikawa, J. R. Chelikowsky, S. G. Louie, F. R. Fischer and M. F. Crommie, *Nat. Nanotechnol.*, 2017, **12**, 1077.
16 K. A. Simonov, N. A. Vinogradov, A. S. Vinogradov, A. V. Generalov, E. M. Zagrebina, G. I. Svirskiy, A. A. Cafolla, T. Carpy, J. P. Cunniffe, T. Taketsugu, A. Lyalin, N. Mårtensson and A. B. Preobrajenski, *ACS Nano*, 2015, **9**, 8997.
17 S. Blankenburg, J. Cai, P. Ruffieux, R. Jaafar, D. Passerone, X. Feng, K. Müllen, R. Fasel and C. A. Pignedoli, *ACS Nano*, 2012, **6**, 2020.
18 Y. C. Chen, D. G. de Oteyza, Z. Pedramrazi, C. Chen, F. R. Fischer and M. F. Crommie, *ACS Nano*, 2013, **7**, 6123.
19 A. Basagni, F. Sedona, C. A. Pignedoli, M. Cattelan, L. Nicolas, M. Casarin and M. Sambi, *J. Am. Chem. Soc.*, 2015, **137**, 1802.
20 L. Lafferentz, V. Eberhardt, C. Dri, C. Africh, G. Comelli, F. Esch, S. Hecht and L. Grill, *Nat. Chem.*, 2012, **4**, 215.
21 J. Eichhorn, D. Nieckarz, O. Ochs, D. Samanta, M. Schmittel, P. J. Szabelski and M. Lackinger, *ACS Nano*, 2014, **8**, 7880.
22 C. Zhang, Q. Sun, H. Chen, Q. Tan and W. Xu, *Chem. Commun.*, 2015, **51**, 495.
23 Q. Sun, X. Yu, M. Bao, M. Liu, J. Pan, Z. Zha, L. Cai, H. Ma, C. Yuan, X. Qiu and W. Xu, *Angew. Chem., Int. Ed.*, 2018, **57**, 4035.
24 Y. Q. Zhang, N. Kepčija, M. Kleinschrodt, K. Diller, S. Fischer, A. C. Papageorgiou, F. Allegretti, J. Björk, S. Klyatskaya, F. Klappenberger, M. Ruben and J. V. Barth, *Nat. Commun.*, 2012, **3**, 1286.
25 H. Y. Gao, H. Wagner, D. Zhong, J. H. Franke, A. Studer and H. Fuchs, *Angew. Chem., Int. Ed.*, 2013, **52**, 4024.
26 Q. Sun, L. Cai, H. Ma, C. Yuan and W. Xu, *ACS Nano*, 2016, **10**, 7023.
27 D. G. de Oteyza, P. Gorman, Y. C. Chen, S. Wickenburg, A. Riss, D. J. Mowbray, G. Etkin, Z. Pedramrazi, H. Z. Tsai, A. Rubio, M. F. Crommie and F. R. Fischer, *Science*, 2013, **340**, 1434.
28 L. Grill, M. Dyer, L. Lafferentz, M. Persson, M. V. Peters and S. Hecht, *Nat. Nanotechnol.*, 2007, **2**, 687.
29 T. A. Pham, F. Song, M. T. Nguyen, Z. Li, F. Studener and M. Stöhr, *Chem. – Eur. J.*, 2016, **22**, 5937.
30 M. O. Blunt, J. C. Russell, N. R. Champness and P. H. Beton, *Chem. Commun.*, 2010, **46**, 7157.
31 U. H. F. Bunz, *Macromol. Rapid Commun.*, 2009, **30**, 772.
32 B. Cirera, Y. Q. Zhang, J. Björk, S. Klyatskaya, Z. Chen, M. Ruben, J. V. Barth and F. Klappenberger, *Nano Lett.*, 2014, **14**, 1891.
33 W. Wang, X. Shi, S. Wang, M. A. Van Hove and N. Lin, *J. Am. Chem. Soc.*, 2011, **133**, 13264.
34 Q. Sun, L. Cai, H. Ma, C. Yuan and W. Xu, *Chem. Commun.*, 2016, **52**, 6009.
35 M. Di Giovannantonio, J. I. Urgel, U. Beser, A. V. Yakutovich, J. Wilhelm, C. A. Pignedoli, P. Ruffieux, A. Narita, K. Müllen and R. Fasel, *J. Am. Chem. Soc.*, 2018, **140**, 3532.
36 Q. Sun, B. V. Tran, L. Cai, H. Ma, X. Yu, C. Yuan, M. Stöhr and W. Xu, *Angew. Chem., Int. Ed.*, 2017, **56**, 12165.
37 L. Cai, X. Yu, M. Liu, Q. Sun, M. Bao, Z. Zha, J. Pan, H. Ma, H. Ju, S. Hu, L. Xu, J. Zou, C. Yuan, T. Jacob, J. Björk, J. Zhu, X. Qiu and W. Xu, *ACS Nano*, 2018, **12**, 7959.
38 J. Liu, Q. Chen, L. Xiao, J. Shang, X. Zhou, Y. Zhang, Y. Wang, X. Shao, J. Li, W. Chen, G. Q. Xu, H. Tang, D. Zhao and K. Wu, *ACS Nano*, 2015, **9**, 6305.

